synthesized with an oligonucleotide that was not complementary to any site in pUC 19, failed to hydrolyze DNA selectively. Neither a 17-nt (**4**) nor an 18-nt (**5**) hybrid nuclease designed to deliver the nuclease to a second site within pUC 19 (Figure 2c) was able to selectively hydrolyze that site. Lack of cleavage may be due to unfavorable secondary structure that prevents hybridization, or to inefficient cleavage of both strands by the bound hybrid nuclease. Simultaneous addition of **4** and **5** to the reaction mixture afforded selective cleavage (fragment sizes ~2120 and ~566 base pairs), possibly because each nuclease was required to hydrolyze only one strand of the duplex. The introduction of additional supercoiling into pUC19 with topoisomerase I and ethidium bromide[15] substantially enhances selective cleavage by hybrid nucleases **2**, **4**, and **5**.

This work illustrates that supercoiled DNA can be sequence-specifically hydrolyzed with a hybrid nuclease delivered via D-loop formation. The hydrolysis is relatively efficient and can be carried out on a preparative scale. The generality of this approach with respect to DNA sequence and structure remains to be determined. Nevertheless, this is an important step toward the development of strategies for cleaving large linear duplex DNAs.

Acknowledgment. Support for this work was provided by the National Institutes of Health (1R01GM41679-01). We also thank the referees for their helpful comments.

(14) Binding domain oligonucleotide: 5'-CTTATTTGGATTGGGAT-3'.
(15) Franklin, P. B.; Schutte, B. C.; Cox, M. M. *J. Mol. Biol.* **1989**, *205*, 487.

Observation of Spin Diffusion in Biomolecules by Three-Dimensional NOE-NOE Spectroscopy

R. Boelens,* G. W. Vuister, T. M. G. Koning, and R. Kaptein

Department of Chemistry, University of Utrecht Padualaan 8, 3584 CH Utrecht, The Netherlands

Received June 12, 1989

The nuclear Overhauser effect (NOE) between two protons is one of the most useful NMR parameters for structural studies of biomolecules in solution.[1] It forms the basis for the methods of sequential resonance assignment in ^{1}H NMR spectra of biomolecules, and it is the source of distance constraints necessary in the structure determination.

For small rigid molecules, the NOE, which is due to dipolar cross-relaxation between the protons,[2] is simply related to the inverse 6th power of the proton-proton distance. Thus measurements of NOE intensities lead in a direct way to relative distances, which can be calibrated by using known distances.[3] However, for large molecules the cross-relaxation pathways via other protons contribute to the NOE between two protons as well.[4] In analogy with similar effects in solid-state NMR, this indirect magnetization transfer is often called spin diffusion.[4,5] Because of the uncertainties due to spin diffusion and the motional behavior of the biomolecule, the NOE is often used to derive just approximate distances.

In the past, several methods have been developed to obtain more accurate distances from NOE data. Instead of recording steady-state NOEs, it was proposed to measure NOE buildup rates after short irradiation times or by transient techniques.[6,7] In the case of biomolecules, the NOE is nowadays generally measured by two-dimensional (2D) NOE spectroscopy,[1,8,9] a method related to the 1D transient technique. Furthermore, for these 2D methods it was preferred to use short mixing times or to use a series of mixing times to extract the initial buildup rate.[10,11] Recently, Olejniczak et al.[12] proposed to irradiate the intermediate spin in the mixing time of a 2D NOE experiment and to estimate in that way the contribution of the indirect magnetization transfer to the NOE. Other approaches used to reduce the effects of spin diffusion are based on the back transformation of the complete NOE matrix, to obtain the relaxation matrix directly.[12,13] For biomolecules, where it is difficult to assign the complete NOE matrix, this procedure can be combined with restrained molecular dynamics to reduce iteratively the effects of spin diffusion.[14]

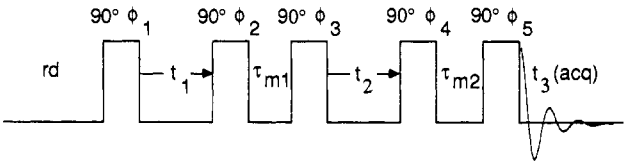

Figure 1. Pulse scheme of the 3D NOE-NOE experiment. Saturation of the HOD line was achieved by low-power irradiation during the relaxation delay, RD, and the two mixing times, τ_{m1} and τ_{m2}. The frequency for the rf pulses and the decoupling was derived from one synthesizer. The phase cycling used is as follows: $\phi_1 = x, -x, y, -y$; $\phi_2 = 2(-x), 2(-y)$; $\phi_3 = 2(-x), 2(-y), 2(x), 2(y)$; $\phi_4 = 2(x), 2(y)$; $\phi_5 = 2(x), 2(-y)$; acq = $x, -x, -y, y, -x, x, y, -y$. TPPI was applied independently for the t_1 and t_2 domains on ϕ_1 and ϕ_3.

Recently, a number of 3D NMR experiments have been reported, such as the homonuclear 3D *J*-resolved experiment,[15] 3D soft COSY-COSY,[16] soft NOESY-COSY,[17] soft NOESY-HOHAHA,[18] nonselective 3D NOE-HOHAHA,[19] HMQC-COSY,[20] and HMQC-NOESY.[20-22] Most of these experiments were motivated by the resulting reduction of overlap on adding a third frequency domain to the 2D NMR spectrum. In addition, as pointed out by Griesinger et al.,[16] the 3D cross-peaks in a COSY-COSY experiment can reveal unambiguously two-step *J* connectivities. Similarly, in the present communication we want to stress the observation of such second-order magnetization transfer for the NOE by the 3D NOE-NOE experiment.

The pulse scheme of the 3D NOE-NOE experiment (Figure 1) reveals two mixing periods separating two evolution periods and a detection period. In each mixing time, the magnetization

(1) Wüthrich, K. *NMR of proteins and nucleic acids*; John Wiley and Sons: New York, 1986.
(2) Solomon, I. *Phys. Rev.* **1955**, *99*, 559-565.
(3) Noggle, J. H.; Schirmer, R. E. *The nuclear Overhauser effect. Chemical applications*; Academic Press: New York, 1971.
(4) Kalk, A.; Berendsen, H. J. C. *J. Magn. Reson.* **1976**, *24*, 343-366.
(5) Abragam, A. *The Principles of Nuclear Magnetism*; Clarendon Press: Oxford, 1961; pp 136-144.
(6) Wagner, G.; Wüthrich, K. *J. Magn. Reson.* **1979**, *33*, 675-680.
(7) Dobson, C. M.; Olejniczak, E. T.; Poulsen, F. M.; Ratcliffe, R. G. *J. Magn. Reson.* **1982**, *48*, 97-110.
(8) Jeener, J.; Meier, B. H.; Bachmann, P.; Ernst, R. R. *J. Chem. Phys.* **1979**, *71*, 4546-4553.
(9) Ernst, R. R.; Bodenhausen, G.; Wokaun, A. *Principles of Magnetic Resonance in One and Two Dimensions*; Clarendon Press: Oxford, 1987.
(10) Kumar, A.; Wagner, G.; Ernst, R. R.; Wüthrich, K. *J. Am. Chem. Soc.* **1981**, *103*, 3654-3658.
(11) Scheek, R. M.; Boelens, R.; Russo, N.; Kaptein, R. *Biochemistry* **1984**, *23*, 1371-1376.
(12) Olejniczak, E. T.; Gampe, R. T., Jr.; Fesik, S. W. *J. Magn. Reson.* **1986**, *67*, 28-41.
(13) Fesik, S. W.; O'Donnell, T. J.; Gampe, R. T., Jr.; Olejniczak, E. T. *J. Am. Chem. Soc.* **1986**, *108*, 3165-3170.
(14) Boelens, R.; Koning, T. M. G.; van der Marel, S. A.; van Boom, J. H.; Kaptein, R. *J. Magn. Reson.* **1989**, *82*, 290-308.
(15) Vuister, G. W.; Boelens, R. *J. Magn. Reson.* **1987**, *73*, 328-333.
(16) Griesinger, C.; Sørensen, O. W.; Ernst, R. R. *J. Magn. Reson.* **1987**, *73*, 574-579.
(17) Griesinger, C.; Sørensen, O. W.; Ernst, R. R. *J. Am. Chem. Soc.* **1987**, *109*, 7227-7228.
(18) Oschkinat, H.; Griesinger, C.; Kraulis, P. J.; Sørensen, O. W.; Ernst, R. R.; Gronenborn, A.; Clore, G. M. *Nature* **1988**, *332*, 374-376.
(19) Vuister, G. W.; Boelens, R.; Kaptein, R. *J. Magn. Reson.* **1988**, *80*, 176-185.
(20) Fesik, S. W.; Zuiderweg, E. R. P. *J. Magn. Reson.* **1988**, *78*, 588-593.
(21) Marion, D.; Kay, L. E.; Sparks, S. W.; Torchia, D. A.; Bax, A. *J. Am. Chem. Soc.* **1989**, *111*, 1515-1517.
(22) Zuiderweg, E. R. P.; Fesik, S. W. *Biochemistry* **1989**, *28*, 2387-2391.

0002-7863/89/1511-8525$01.50/0

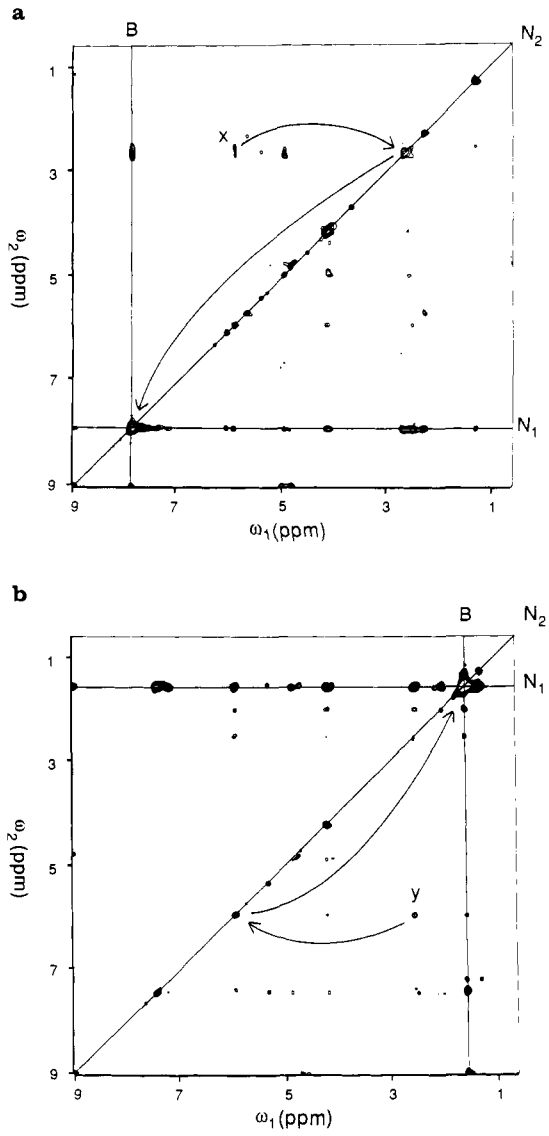

Figure 2. Two ω_1/ω_2 cross-sections taken from the 500-MHz 3D NOE–NOE spectrum of 5 mM 22-bp symmetric *lac* operator in ^2H_2O, 50 mM KP_i, 200 mM NaCl, pH 6.5, 27 °C. The cross sections were taken at the ω_3 frequencies of the G5 H8 proton (a) and of the T8 H_2'' proton (b). The lines indicated with N1, N2, and B are the intersection of the cross sections with the diagonal NOE planes and the back-transfer plane. The two-step NOE transfers indicated with x and y are explained in the text. The spectrum was recorded with two dummy scans and eight scans and resulted in a real 200*224*512 data matrix in the t_1, t_2, and t_3 dimension, respectively. Both mixing times were equal and taken to be 200 ms. Sixty degree shifted sinebell (t_3) and Hamming (t_1 and t_2) window multiplications were used. Zero filling was used in the t_1 and t_2 dimension to yield a real 3D spectrum of the size 256*256*256. An automatic third-order-polynomial base-line correction was applied on the three domains. The data were processed with our 2D NMR processing software, optimized for fast data access in all domains.[19]

of one spin is transferred with a certain efficiency to another. Assuming indirect transfer to second order, we obtain for the NOE intensity

$$a_{ij} = -\sigma_{ij}\tau_m + \tfrac{1}{2}(\Sigma'\sigma_{il}\sigma_{lj})\tau_m^2 \quad (1)$$

where τ_m is the mixing time and σ_{ij} the cross-relaxation rate between spins i and j. The 3D cross-peak intensity is proportional to the product of both transfer efficiencies

$$a_{ijk} = a_{ij}a_{jk} = (\sigma_{ij}\sigma_{jk})\tau_m^2 \quad (2)$$

in a first approximation and when both mixing times are the same. It is clear that in that case the 3D intensity is identical with one term of the second-order transfer in eq 1. Thus the 3D NOE–NOE experiment can trace specific spin-diffusion pathways, while in 2D cross-peaks, only the sum of all pathways is observed and it is often impossible to dissect this sum into the various contributions because of overlap.

Of course, magnetization transfer in the mixing periods is usually incomplete. This results in intensity accumulating on the body diagonal and two cross-diagonal NOE planes in the 3D spectrum, as pointed out previously for the 3D NOE–HOHAHA spectrum.[19] Furthermore, magnetization transferred forward in the first mixing time can be transferred backward in the second period over the same pathway. This leads to intensity on a third diagonal plane, the so-called back-transfer plane.[17,19] However, all intensity outside these three planes can be ascribed to at least double magnetization transfer. Of course, for long mixing times τ_m there may be contributions of spin diffusion to 3D cross-peaks as well.

The pulse train of Figure 1 was applied to a symmetric 22-bp *lac* operator fragment.[23,24] The experiment took 137 h, 29 h of which was required for I/O operations. By using field gradient pulses in the mixing times instead of phase cycling for the NOE selection, a further time reduction should be possible. Although one might expect problems with instrumental stability over such prolonged measurements, no serious t_1/t_2 noise artifacts were observed in the resulting 3D spectrum. As an example, Figure 2 shows two slices from the 3D spectrum perpendicular to the ω_3 axis, taken at the resonance frequencies of the aromatic H8 proton of G5 and the methyl group of T19. Three lines are indicated in the spectrum, which represent the intersection of the slices with the diagonal planes. On lines N1 and N2 are found the direct NOEs due to the first and second mixing times, respectively, while line B reveals the weaker two-step back transfer via the other spins. The many cross-peaks outside these three lines are all indicative of double magnetization transfer. Thus, the peak marked with x in Figure 2a shows that a spin-diffusion pathway exists from G5 H_1' via G5 H_2' to G5 H8, while peak y in Figure 2b demonstrates the transfer from T19 H_2'' via T19 H_1' to the T19 methyl group. The results emphasize the contribution of spin diffusion to the NOE in large biomolecular systems. The 3D NOE–NOE experiment reported here could be used to estimate the various contributions to indirect magnetization transfer and thus to obtain more accurate values for the cross-relaxation rates. The 3D cross-peak intensities could be quantitated by summation of all intensity present in a volume around the cross-peak. In this way the various contributions of first-order spin diffusion (cf. eq 2) could be determined. Due to the large number of 3D cross-peaks observed (about 10000), some tools for automation are highly desirable. The reduced overlap is then an advantage, since relatively simple algorithms can be used for peak extraction.

Another feature of the present nonselective 3D NOE–NOE experiment is the reduction of overlap in complex ^1H NMR spectra. This could be extremely useful for obtaining a large number of distance constraints, which is crucial for accurate structure determinations by NMR.[1] It could push the size of biomolecular systems amenable for structural NMR studies beyond the present limit of ca. 15 kDa. In fact the method is very suitable for studying large biomolecules, since it is not based on possibly small homonuclear J couplings and cross-relaxation becomes more efficient with larger molecular weights.

Acknowledgment. This research was supported by the Netherlands Foundation for Chemical Research (SON) with financial aid of the Netherlands Organization of Scientific Research (NWO). We thank Dr. J. H. van Boom for the synthesis of the *lac* operator fragment and D. Schreurs for writing the software for display of 3D NMR data on an Evans and Sutherland PS300 picture system.

(23) Scheek, R. M.; Boelens, R.; Russo, N.; Kaptein, R. In *Structure and Motion: Membranes, Nucleic Acids and Proteins*; Clementi, E., Corogui, G., Sarma, M. H., Sarma, R. H., Eds.; Adenine Press: Guilderland, NY, 1985; pp 485–495.

(24) Lamerichs, R. M. J. N.; Boelens, R.; van der Marel, G. A.; van Boom, J. H.; Kaptein, R.; Buck, F.; Fera, B.; Rüterjans, H. *Biochemistry* **1989**, *28*, 2985–2991.